Analysis of Energy Consumption for electric motorcycles depending on vehicle configuration and driving cycles

Analysis of Energy Consumption for electric motorcycles depending on vehicle configuration and driving cycles

A Niccolai*, L Berzi, F Barone, N Baldanzini

Department of Industrial Engineering (DIEF), University of Florence, Via di S. Marta, 3, 50139, Florence, Italy.

* e-mail: adelmo.niccolai@unifi.it

Abstract. This article presents an analysis of energy consumption for battery electric motorcycles (BEM) based on vehicle configuration and driving cycles. The study investigates the impact of two architectures: rear-wheel regenerative (RWR), and two-wheel regenerative (2WR) on consumption. For the analysis, the study considered the effect of various parameters on the longitudinal vehicle dynamics such as speed profiles (WMTC, real-world profile), longitudinal road slope (from -5° to 5° with 0.5° step increment), and 5 different brake distributions. The research employs simulation techniques using the Matlab/Simulink environment to develop a simplified longitudinal vehicle dynamics model (1 DOF) and for the implementation of a serial brake-blending control strategy. The results of the analysis provide energy potential regeneration and insight into the sensitivity of energy consumption to road slope variations, powertrain working points, and potential energy harvesting. The findings contribute to a valuation of the factors that influence energy consumption in electric motorcycles and have implications for the development of vehicle architectures through accurate range assessment on real-world riding conditions and provide valuable information for powertrain components right-sizing.

1. Introduction

The electrification of road transport is one of the strategies adopted to reduce or mitigate mainly the CO_2 emission related to road vehicles [1]. In the last years, also due to the nudging by the policy maker, an increment of electric vehicles in terms of units produced and sold has occurred [2].Furthermore, analysis and study predict the growth of these types of vehicles in the next year [2]. The characteristics of the electric powertrain such as the high torque offered at zero speed of the electric machine, and the lower energy density of the battery than the fossil fuels influence the vehicle design. This latter type of vehicle needs/allows different architectures than the conventional vehicles. Thus, a rethinking of the vehicle design is necessary, especially for motorcycles due to the smaller volume or size than the car. The battery capacity and vehicle mass are closely related, and an increment of the vehicle mass means also an increment on consumption [3]. A reduction of the battery capacity without changes the drive range, for example via regenerative braking, would be ideal. The aim of this study is to investigate *unusual* configurations that could play a pioneering role in further developments. A big difference between conventional vehicles and electric vehicles is the possibility of recovering energy by operating the electric machine as a generator, although the presence and use of a mechanical braking system is still needed for technical and safety reasons [4]. The two architectures investigated by the authors were the rear-wheel regenerative configuration (RWR) and the two-wheel regenerative configuration (2WR). The braking regeneration was achieved by a single electric machine for the RWR and by two, one for each

axle, on the 2WR to allow better braking behaviour [5]. The traction was always provided by the rear motor. In this work, many aspects of the 2WR configuration were not investigated such as the increment of the unsprung masses, wheel inertia, and steering inertia. The focus was to determine the influences on consumption which is obviously a single aspect of the entire powertrain puzzle, aimed to help in the choice of the vehicle architecture.

2. Materials and Method

This section describes the materials and methods used in the work. In the first subsection, the vehicle models and speed profiles were introduced, and then the braking distribution and braking control strategy were explained in the second subsection. In the last subsection, the methodology and simulation outputs were defined.

2.1 Vehicle Model and Speed Profiles

For the analysis of the vehicle architectures and an estimation of the consumption, a simplified motorcycle model was developed. The simulation environment Matlab/Simulink was utilized for this scope. The vehicle model, based on in-plane vehicle dynamics (1 DOF), was comprehensive of the mechanical and electrical system (powertrain), the rider (speed profiles controller), the environment (road grades), and the braking strategy. The two configurations (RWR, 2WR) shared the same component for the rear wheel powertrain which consists of a permanent magnet synchronous machine, transmission (single gear ratio), final chain transmission, and battery. For the 2WR architecture, an additional wheel hub motor was implemented in the front wheel, increasing also the vehicle mass of 15 kg in this configuration. The total mass, including the rider mass, was 370 kg for the RWR architecture. A schematic representation of the 2WR architecture is shown in Figure 1.

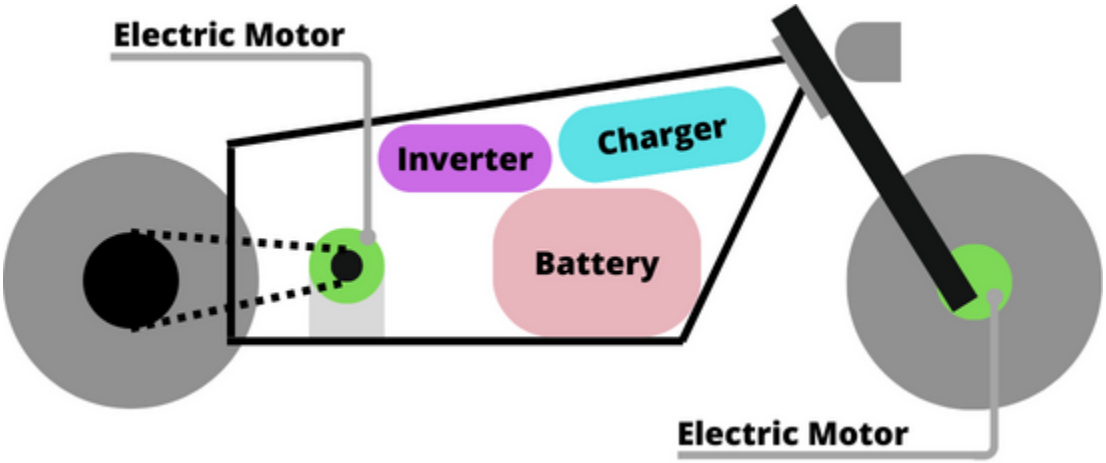

Figure 1: A simple scheme of two-wheel driven electric motorcycles. The rear motor torque is supplied to the rear wheel via a chain transmission, while the front motor is implemented directly in the front wheel hub.

All the vehicle parameters for the calculation of driving resistance were kept constant for the whole simulation and based on literature values. The product of front cross section area and drag coefficient is 0.35, and rolling coefficient is 0.013. The vehicle model neglects many aspects like the tire slip, the influence of suspension, the lateral dynamics, and other aspects that might influence the consumption; the efficiency of the powertrain group is based on a typical PMSM machine, a technology typically suitable for motorcycle application. Despite these limitations, a control on adhesion longitudinal coefficient and wheelie was implemented to avoid possible unphysical phenomena. The two speed profiles are shown in Figure 2. The first one is the WMTC speed profiles while the second one was obtained by processing of naturalistic riding in a mixed urban and rural trip (Firenze-Bologna on open

roads) using an electric motorcycle whose size is comparable to the simulated one; therefore, such real-world data are considered a typical case study for the vehicle class under analysis.

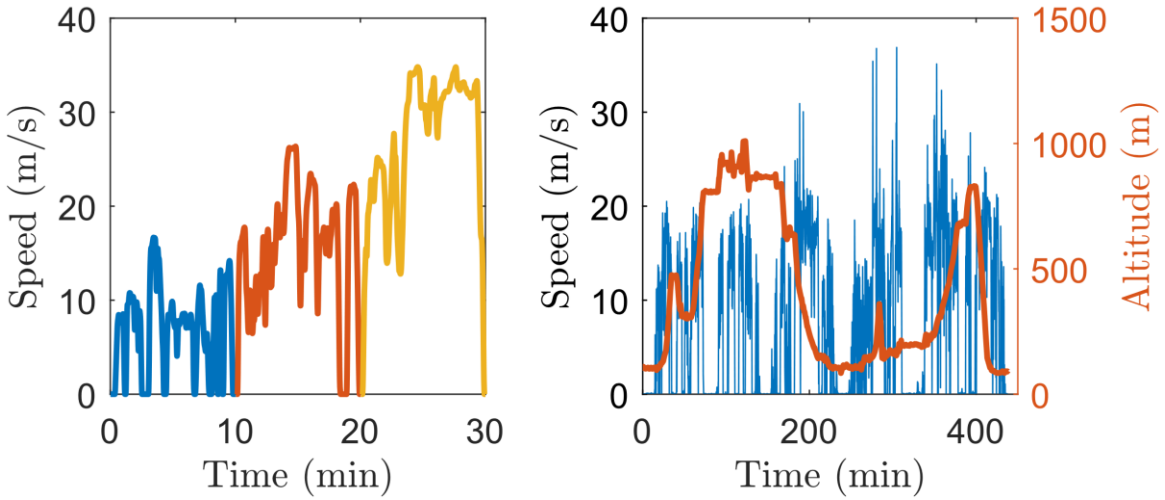

Figure 2: shows the vehicle class 3 WMTC speed profile on the left subplot. Only part 2 was used for the analysis (colored in orange). On the right subplot is displayed the speed and altitude signals recorder during a motorcycle trip and used for the creation of the experimental driving cycle.

The WMTC part 2, class 3, subclass 2 was chosen because is the standard for test homologation of motorcycles with a maximum vehicle speed bigger or equal to 140 km/h [6]. The average driving speed is 58.8 km/h (WMTC) and 48.6 km/h (experimental), and the maximum speed is 94.9 km/h (WMTC) and 133 km/h for the other speed profile. The two cycles have a standard deviation of acceleration value of 0.68 m/s^2 (WMTC) and 0.76 m/s^2 (experimental). Finally, the WMTC has a difference in altitude of zero meters while the other speed profile has a maximum altitude variation of 926 meters.

2.2 Brake distribution and Brake-blending

Electric motors can also work as a generator to recover the vehicle's kinetic energy during the braking manoeuvres. The two main aspects that influence the braking performance in the simplified model were the braking distribution (ρ), and the brake-blending strategy. These latter variables describe the braking force axle repartition, and the brake axle force splitting between the friction brakes and the regenerative brakes, respectively. The braking distribution (ρ) was defined in equation (1), where X_R is the rear axle brake force, and X_F is the front axle brake force.

$$\rho = \frac{X_R}{X_R + X_F} \quad \#(1)$$

The variable (ρ) ranges from 0 (no rear brake) to 1 (only rear brake). The braking distribution was kept constant from the beginning to the end of the simulations, but it was changed between different runs, and it belongs to the following set: $\boldsymbol{\rho} = \{0, 0.25, 0.5, 0.75, 1\}$. In order to increase the energy regeneration, a serial control strategy was implemented for each axle [7], albeit it means a worse and less safety adherence coefficient allocation with potential issues at high deceleration [4]. This latter strategy first splits the braking torque request between the two axles, then aims to demand the maximum regenerative torque allowed by the motor, and then the remaining braking torque request is added by the frictional/dissipative brakes as done in previous work [8]. The feasibility of the braking system or the possibility of implementing wasn't considered in this work, but the focus was the outcomes in terms of energy and regenerative braking. The brake-blending strategy, for the RWR architecture, was defined by equation (2), while the graphic representation of the logic for the 2WR architecture is shown in Figure 3.

$$F_{brake} = \{F_{reg}, \quad F_{brake\_request} \leq F_{reg\_max}\ F_{reg\_max} + F_{friction}, \quad F_{brake\_request} > F_{reg\_max} \quad \#(2)$$

Where F_{brake} is the braking force required by the rider, F_{reg} is the regenerative force applied by the motor, F_{reg_max} is the maximum force value allowed by the motor due to mechanical and operational limits, and $F_{friction}$ is the force supplied by the frictional brakes.

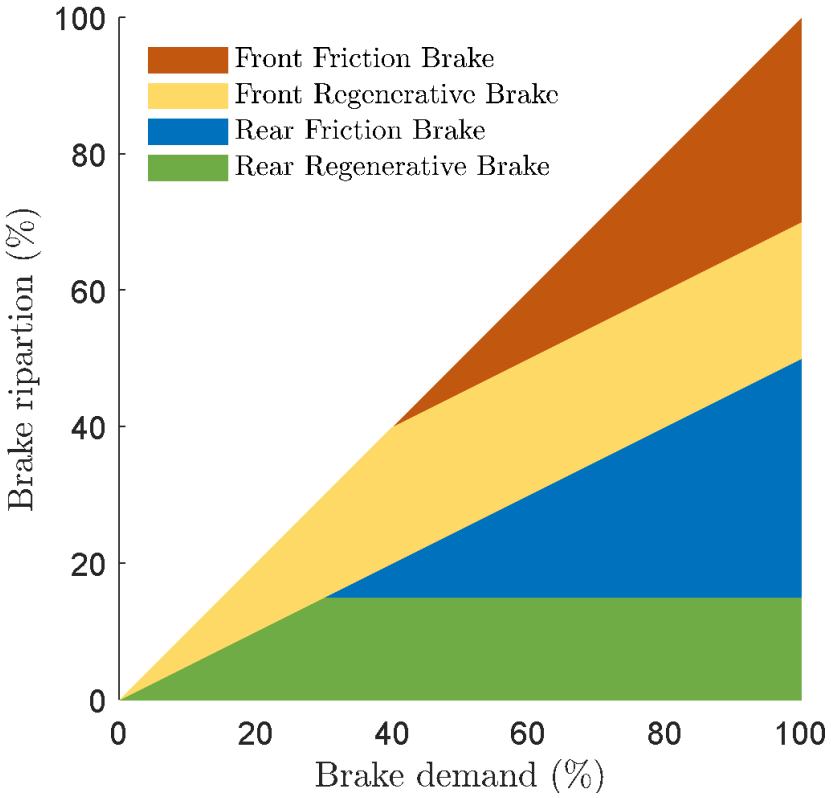

Figure 3: shows the brake serial control strategy for a two-wheel regenerative electric motorcycle (ρ = 0.5). Highlighted areas represent the cumulative braking force for each type of brake device.

The action of braking was implemented via blending the two types of braking (regenerative, and dissipative), independently of the rider's actions. The brake lever feedback of a hypothetical rider will not be affected during the braking manoeuvres because the rider brake demand was guaranteed with different combinations of the brakes without changing the output (total brake force).
Finally, for both architectures, the torque needed for the traction was supplied only by the rear motor for simplicity given the aim of studying the braking energy and regeneration.

2.3 Method

Multiple vehicle simulations were performed to evaluate how the different powertrains, driving cycles, and braking parameters have an influence on consumption. Investigation of the powertrain components was conducted by switching from the two architectures (RWR, 2WR), changing the braking distribution value (for a total of five values), and changing the drive profile (WMTC, experimental). In addition, an analysis of the road slope influence on operation point and energy flow was conducted, adding altitude profiles at the WMTC speed profile to evaluate the influence of the road slope on consumption [9]. The altitude profiles were obtained considering a constant road slope angle (α) for the whole distance travelled by the vehicle. This latter variable ranges from minus five to five degrees with incremental steps of a half degree. The modified speed profiles are shown in Figure *4*.

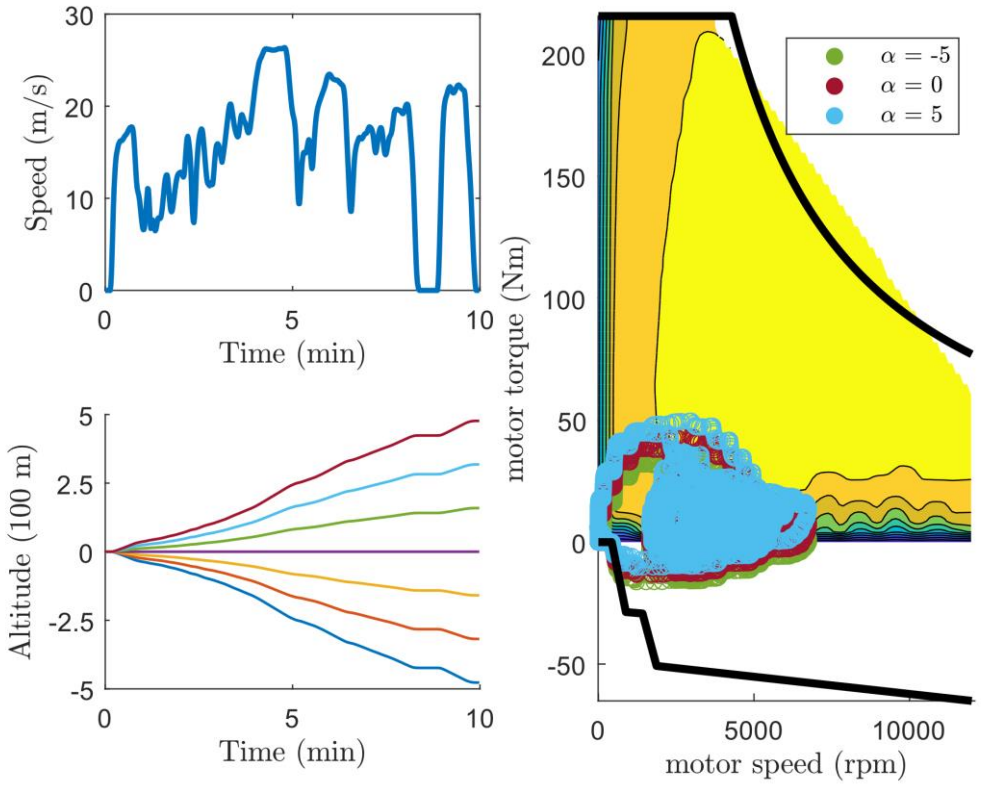

Figure 4: In the top right subplot is plotted the WMTC speed vs. time signal. In the bottom left subplot, different altitude profiles are shown for different constant road slope values. On the right subplot the operation points for three different road slope angles.

The net energy, average motor efficiency, and equivalent energy were used for each simulation to compare the different vehicle configurations and speed profile results. Net Energy was defined as the difference between supplied battery energy and the regeneration energy, at the battery, normalized by the distance travelled by the vehicle as described in equation (3).

$$\underline{E} = \frac{E_{battery_{out}} - E_{battery_{in}}}{distance} \quad \#(3)$$

Average motor efficiency was defined as the mean efficiency of the electric motors (only rear, to a fair comparison between architectures) achieved during all the operations (traction and braking), using a look-up table depending on RPM and torque, equivalent to a typical PMSM efficiency, as said. *Equivalent energy* is the net energy minus the normalized potential energy by the distance, and it is the energy spent by the vehicle considering a zero net altitude but with a different efficiency of the powertrain. With these parameters were possible to compare results obtained by different boundary and initial condition, input data, and vehicle configuration.

3. Results

In the first subsection, how the braking distribution and braking-blending control strategy influence consumption is shown. The influence of road slope on the motor operative points and consumptions is provided in the second subsection.

3.1 Regenerative braking for vehicle configurations

The results obtained for the two driving cycles (WMTC, experimental) and the architectures (RWR, 2WR) are shown in Figure 5.

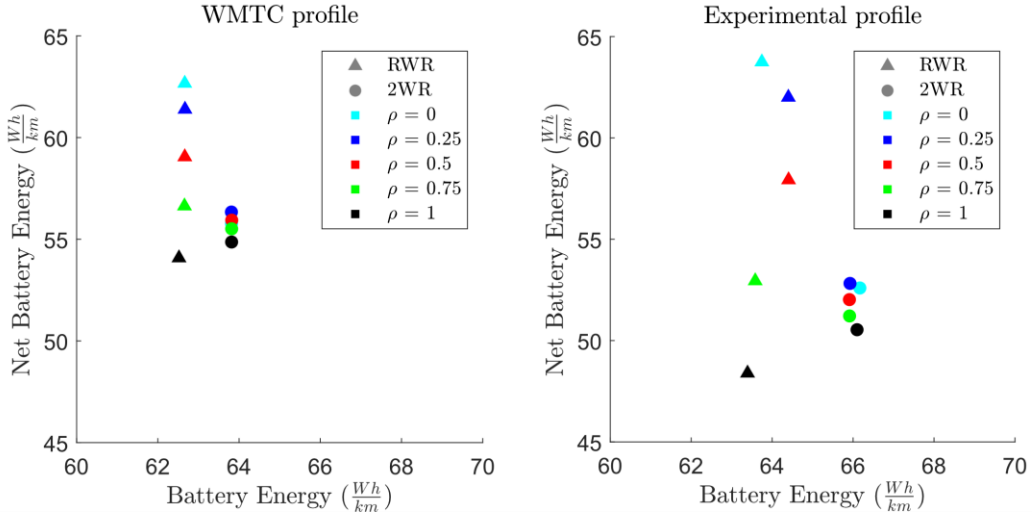

Figure 5: shows the results for the speed profiles, WMTC and the experimental, on the right and left subplots respectively. The geometric dot shape (triangle, circle) means the vehicle configuration (RWR, 2WR). Different colors mean different braking distribution values (see the legend for the details).

The RWR configuration had a normalized energy request of 62.6 Wh/km and 63.9 Wh/km for the WMTC and experimental profiles respectively. The 2WR energy demand was 63.8 Wh/km and 66 Wh/km for the same cycle list. When the braking distribution was equal to one the lowest consumptions were obtained for all the vehicle architecture (RWR, 2WR) and speed profiles (WMTC, experimental). The minimum value of the 2WR was always higher than the minimum value of the RWR configuration. The maximum value for the RWR configuration was obtained always for ρ equal to zero (no regeneration at all). The 2WR maximum was obtained for ρ equal to 0.25 in both cycles ($\rho = 0$ means only front regeneration). The RWR consumption ranges from 54.1 to 62.7 Wh/km and from 48.4 to 63.8 Wh/km for the WMTC and experimental profiles respectively. While the 2WR configuration ranges from 54.9 to 56.3 Wh/km (WMTC profile) and 50.5 to 52.8 Wh/km (experimental profile).

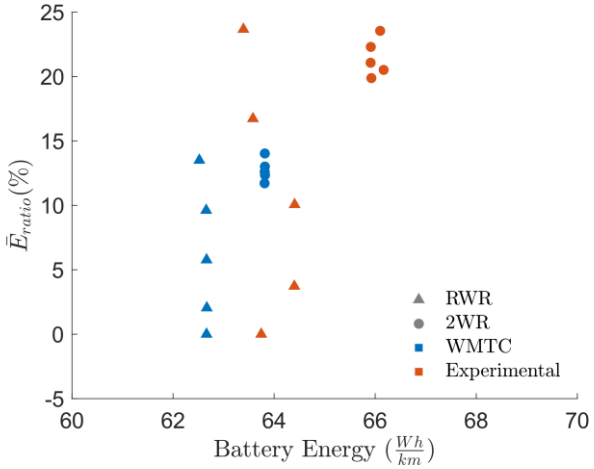

Figure 6: shows the energy ratio for different configurations and speed profiles. The geometric dot shape (triangle, circle) means the vehicle architecture configurations (RWR, 2WR) while the dot color (blue, orange) means the speed profile (WMTC, experimental).

The energy ratio, described as the ratio between the regenerated energy and the delivered energy, is shown in Figure 6. The minimum ratio value (0%) was obtained for the RWR in the case of no regeneration ($\rho = 0$) independently of the driving cycle. The 2WR configuration has a minimum of 11.7 % (WMTC profile) and a maximum of 23.6 % (experimental profile), while the maximum ratio was 23.7 % for the RWR-WMTC combination.

3.2 Road slope influence

As described in subsection 2.3, an analysis of the road slope influence on consumption was performed by adding altitude profiles at the WMTC speed profiles (constant road slopes, see Figure 4 for some examples). The net energy results for the two configurations are shown in Figure *7*, RWR on the left subplot and 2WR on the right subplot.

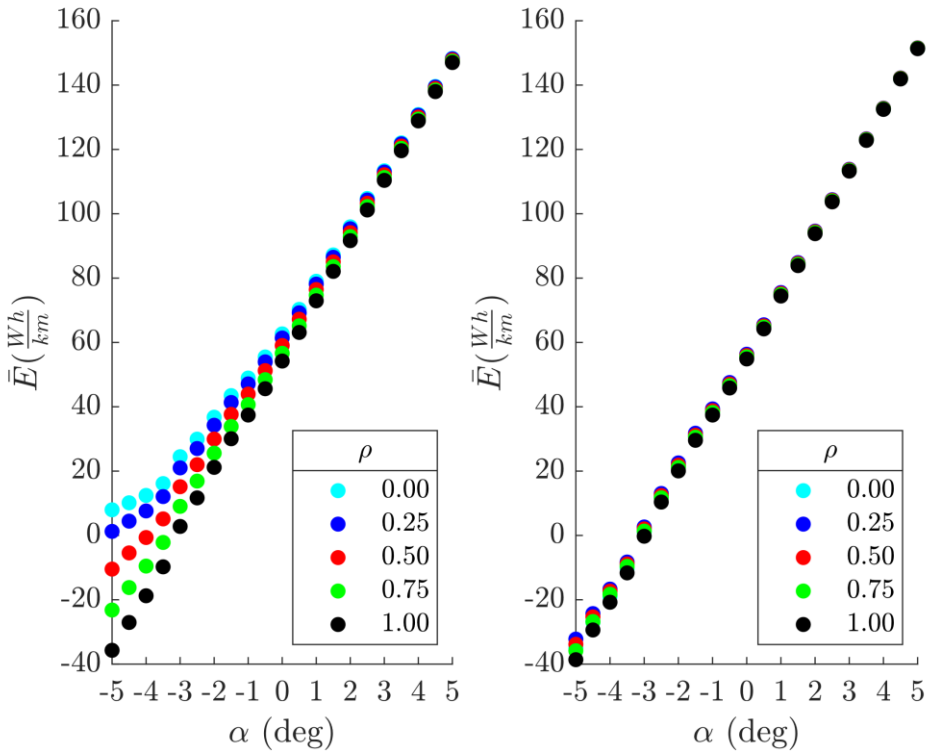

Figure 7: shows the net energy for the RWR on the left subplot and the 2WR on the right subplot for five values of the braking distribution (ρ).

For positive road slope values (uphill direction) the net energy was less influenced by the braking distribution value. In the downhill direction (negative alpha values), variation of ρ affects more the net energy, and in the case of 2WR, it was always negative for all the ρ values. At minus five degrees, for the WMTC profile, the net energy range was 43.7 Wh/km (RWR) and 5.1 Wh/km (2WR). The maximum consumption was 148.3 (RWR) and 151.6 Wh/km (2WR) at alpha equal to five degrees and changing the braking distribution, reduce consumption of 1.3 and 0.3 Wh/km (RWR, 2WR) at maximum. With the addition of the road slope, there is also an additional demand for energy (potential energy) and so on consumption. Thus, to evaluate the architecture performance at the net energy, the normalized potential energy was subtracted from it (called as equivalent energy in subsection 2.3). This latter *new energy* and the average rear motor efficiency are displayed in Figure 8 for the modified WMTC profile. Higher was the road angle and higher was the average rear motor efficiency for all the configurations and braking distribution values. Furthermore, looking at the RWR results, the difference between the net energy and the normalized potential energy decreased for ρ equal to 0 and 0.25 and increases for the other values. While for the 2WR with positive road grades, the increment was always bigger than with

zero road angle. The efficiency of the rear motor increased with positive angles in both vehicle configurations, while it had a non-monotonic trend for negative alpha values (increasing and decreasing).

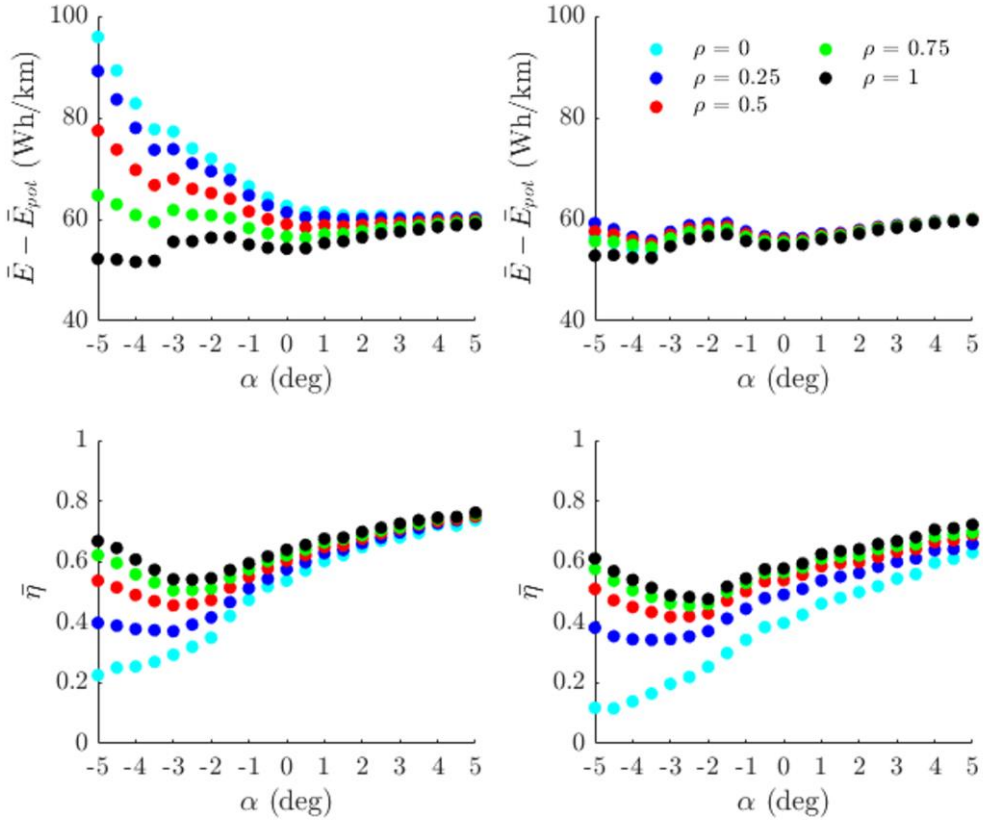

Figure 8: the two top subplots show the net energy minus the potential energy normalized by the distance for the two vehicle configurations (RWR on the left and 2WR on the right). In the two bottom subplots, the average rear motor efficiency is displayed.

4. Discussion

In this section, a discussion of the results is provided. In the first subsection, the diversity of consumption for the two architectures is threatened. The second subsection focuses on the road slope's influence on consumption.

4.1 Architectures influence

The 2WR had always the highest energy demand (63.8 and 66 Wh/km) in both cycles (WMTC, experimental) than the RWR, due to the mass increment given by the front motor. The RWR had the lowest consumptions (54.1, 48.4 Wh/km) in each driving cycle when ρ was equal to one (only rear braking force). Setting ρ = 0 could also be seen, energetically speaking, as a strategy where the regenerative rear brake is saturated, and then the other braking power is supplied by frictional brakes (front or rear). The worst consumption results (56.3, 52.8 Wh/km) for the 2WR were obtained for rho equal to 0.25 but they were lower than the second better result of the RWR (at ρ = 0.75). The 2WR with ρ = 0 (only front braking regeneration) performed a little better than 0.25 braking distribution. With ρ equal to one the 2WR vehicle had higher consumption than the RWR with the same braking distribution value, due to the energy losses inducted by the mass increment such as the tire rolling resistant moment and the not unitary powertrain efficiency (impossibility of recovering all the energy). This result was still the better result of the 2WR even if the front motor does not recover energy. The RWR consumption

was reduced, compared to the non-regenerative case (RWR, $\rho = 0$) of 13.6% (WMTC, $\rho = 1$) and 24.1% (experimental, $\rho = 1$). The 2WR reductions were of the 12.4% (WMTC) and 21% (experimental). While the worst results were 2% (WMTC, $\rho = 0.25$) and 2.7% (experimental, $\rho = 0.25$) for the RWR. The 2WR architecture obtained 10.1% (WMTC, $\rho = 0.25$) and 17.14% (experimental, $\rho = 0.25$) as worst consumption reductions, which were more than three times bigger than the RWR worst results. The lower energy recovery results on WMTC than the experimental profile was related to the lower energy dissipated via braking, rather than air drag and rolling resistance, so the braking regeneration influenced less the consumption due to the speed profile nature. Looking at the energy ratio, the conclusions are the same as made for the net energy, in fact, the energy ratio is equal to one minus the ratio between the net energy and the supplied energy.
The final energy consumption of the 2WR was less sensitive to the braking distribution in comparison with the RWR; due to the increased mass however, the absolute value was comparable or higher. Considering braking distribution with the prevalence on the front axle the potential energy consumption reduction due to regeneration was estimated to be remarkable, from 2.7% (experimental profile, RWR, rho = 0.25) to 17.1% (experimental, 2WR, rho = 0.25). Therefore, for these speed profiles (moderate deceleration, coherently with naturalistic riding on open roads and with WMTC values) a solution with only a rear braking regeneration is assessed to be the optimal solution for energy regeneration and consumption but it might be not for a safety allocation of the longitudinal adherence coefficient (road slippery condition or influence the ABS activation).

4.2 Road slope influence

An increment of the net energy by adding a positive road slope was trivial because, for the same speed profile, it was added a request of more energy (potential energy). As well as a decrement with negative α values. Interesting was the relative increment/decrement of net energy (+136 %/-87.3%, $\alpha = 5/-5$) which was more than the potential energy itself because of the non-unitary efficiency of the powertrain. With positive slope angles, the influence of the braking distribution on consumption was neglectable for both architectures because of the same deceleration (same speed profile) the braking force was mainly supplied by the force of gravity component parallel to the road (decrement of the braking force). While a lower longitudinal road angle meant a higher difference in net energy for different ρ, especially for the RWR configuration. The average rear motor efficiency (Figure 8) increased with the increment of positive α values, thus the motor worked at an overall higher average efficiency (higher in traction and lower in braking) than the zero-altitude profile. Instead with a negative road slope, the efficiency decreases until a local minimum between -2 and -3 degrees and then increased again due to the limit of braking regeneration (motor cut-off). Positive α values reduced the ρ independency on the equivalent energy because the tire forces were mainly positive (traction). For a certain value of α or bigger there are no braking tire forces at all, thus the equivalent energy convergence to a unique value, independently by the ρ variable. Vice versa for negative road slope values the braking tire forces increase and ρ influences strongly the results, especially for the RWR configuration. In fact, even if the average rear motor efficiency had similar behaviour in both vehicle configurations (Figure 8, two bottom subplots), the equivalent energy (Figure 8, two top subplots) and net energy (Figure 7) were less affected for 2WR vehicle by the choice of ρ because of the front motor efficiency increment.

5. **Conclusion**

In this work, the influence on the consumption of two fully electric motorcycle architectures was investigated via two different speed profiles, five braking distribution values, and a serial control braking strategy. In addition, the influence of the road slope was analysed by adding altitude profiles at the WMTC speed profile. Results suggested that the rear wheel regenerative (RWR) architecture is preferable (less consumption, much simpler, and cheaper) if it is possible to apply a logic where the rear regenerative torque is prioritized ($\rho = 1$). The 2WR benefit of an almost braking distribution independence on energy reduction. This latter configuration could be better in situations where high decelerations and high adhesion coefficient are required, thus the investigation via harsh driving cycle

could be worthy. The energy dissipated by the brakes (regenerative and frictional) was the same for the same cycle and vehicle configuration. Thus, the only rear wheel regeneration must be preferred with low deceleration and not harsh application such as moped, due to the less vehicle mass, complexity, and cost. The 2WR, despite the complexity increment, could be a solution for "sport" driving cycles because the ρ independence allows it to regenerate with the front or rear wheel proportional to the braking request. Furthermore, two motors could allow for the optimization of the traction phases that were not studied in this work. On the other hand, adding mass and moment of inertia to the front assembly influences the vehicle handling so a different setup (caster angle, normal trail, etc.) could be necessary for this type of vehicle. An analysis of the road slope was conducted, even with all the limitations of adding a posteriori altitude profile on a speed profile. The results showed that consumption obviously increased (uphill direction) and decreased (downhill direction) but road slope has also an influence on the operative points. The efficiency (not unitary) of the powertrain even for an altitude profile with zero potential energy implicates an increment of consumption and neglected the road slope at all is a simplification, especially for the RWR configuration. The road slope acts by transferring the weight from one axle to the other (uphill or downhill direction) shifting the braking force consequentially, so a 2WR configuration could be preferable to avoid wheel locking. More detailed studies for harsh cases and more architectures, and considering the legal constraint, should be made to clarify if the increment of mass and complexity fulfilment the energy reduction otherwise is better to invest in vehicle development of other solutions such as mass reduction, tire improvement, and powertrain efficiency optimization.

References

[1] European Commission, 2017 European Roadmap Electrification of Road Transport Status: final for publication
[2] - International Energy Agency I 2023 Global EV Outlook 2023: Catching up with climate ambitions
[3] Weiss M, Cloos K C and Helmers E Energy efficiency trade-offs in small to large electric vehicles
[4] Oleksowicz S, Ruta M, Burnham K, Curry E and Garces H 2013 Legal, safety and practical regenerative braking control challenges *Measurement and Control (United Kingdom)* **46** 283–8
[5] Spichartz P, Bokker T and Sourkounis C 2017 Comparison of electric vehicles with single drive and four wheel drive system concerning regenerative braking *2017 12th International Conference on Ecological Vehicles and Renewable Energies, EVER 2017*
[6] European Commission, 2019, Regulation No 134 of the Economic Commission for Europe of the United Nations (UN/ ECE) — Uniform provisions concerning the approval of motor vehicles and their components with regard to the safety-related performance of hydrogen-fuelled vehicles (HFCV) [2019/ 795]
[7] Qiu C, Wang G, Meng M and Shen Y 2018 A novel control strategy of regenerative braking system for electric vehicles under safety critical driving situations
[8] Yuan Y, Zhang J, Li Y and Li C 2018 A Novel Regenerative Electrohydraulic Brake System: Development and Hardware-in-Loop Tests *IEEE Trans Veh Technol* **67**
[9] Björnsson L-H and Karlsson S 2016 The potential for brake energy regeneration under Swedish conditions